Synthesis and Characterization of Long Chain Branched Isotactic Polypropylene via Metallocene Catalyst and T-Reagent

Justin A. Langston, Ralph H. Colby, and T. C. Mike Chung*

Department of Materials Science and Engineering, The Pennsylvania State University, University Park, Pennsylvania 16802

Fumihiko Shimizu, Toru Suzuki, and Masaru Aoki†

Mitsubishi Chemical Group, Science and Technology Research Center, Inc., 1000 Kamoshida-cho, Aoba-ku, Yokohama 227-8502, Japan

Received September 11, 2006; Revised Manuscript Received January 26, 2007

ABSTRACT: Long chain branched isotactic polypropylenes (LCBPP) prepared via the combination of *rac*-Me_2-Si(2-Me-4-Ph-Ind)$ZrCl_2$/MAO catalyst and a *p*-(3-butenyl)styrene (T-reagent) were characterized to investigate their synthesis, structure, solution properties, and melt properties. The T-reagent, in the presence of hydrogen, simultaneously served as a comonomer and chain transfer agent, resulting in a LCBPP with high molecular weight, desirable branch point density, and relatively well-defined molecular structure. Additionally, the metallocene catalyst remained highly reactive. To understand the structure−property relationships, a series of LCBPPs were prepared with similar weight-average molecular weights of about 250 000 g/mol and different branch densities ranging from 0 (linear iPP) to 3.3 branch points per 10 000 carbons. ^{1}H NMR and SEC equipped with triple detectors revealed structural information. Melt properties were examined by small-amplitude dynamic oscillatory shear and extensional flow measurements. LCBPPs of similar molecular weights displayed a systematic increase in zero-shear viscosity and Arrhenius flow activation energy as branch density increased. LCBPPs with high branch point density displayed thermorheologically complex behavior. Strain hardening was observed in extensional flow of LCBPPs.

Introduction

Long chain branched (LCB) polymers have value in processing techniques which demand high melt strength, including thermoforming, film blowing, extrusion coating, and blow molding processes.[1] Within the polyolefin family, polyethylenes have received much attention with respect to the many types of branching, while polypropylenes have gained much less attention. This lack of attention is due to the difficulties in preparing branched polypropylenes, particularly those with well-defined structure. Difficulties in creating branched polypropylenes arise from the limited chemistry to produce highly isotactic polypropylenes. These chemistries include Zeigler−Natta and metallocene catalysis which produce highly linear and highly stereospecific polymers. Although these catalysts produce polypropylenes with desirable properties, they are extremely sensitive to functional comonomers and traditionally cannot produce a branched structure. As a result, polypropylene has been limited in some end uses.

Difficulties in the synthesis of branched polypropylenes have led to increased interest in chemical modification of polypropylene. Among the most successful have been reactive extrusion[2,3] and electron beam irradiation[4−6] which degrade the polypropylene in a controlled fashion to create branches. These techniques have previously been used to prepare branched polymers with increased zero-shear viscosities, broadened relaxation spectra, and strain hardening behavior,[7−9] but the structures have only been partially characterized. This lack of structure characterization is in part due to the complicated nature of the materials. Reactive extrusion and electron beam irradiation techniques create branched polymers with broadened molecular weight distributions and a complex distribution of structures.

Direct synthesis of long chain branched isotactic polypropylenes (LCBPP) has been limited. The incorporation of polypropylene macromonomers has been studied utilizing various techniques. In situ formation of polypropylene macromonomers has been studied by the use of a single metallocene catalyst[10] and the use of tandem catalysis.[11] Additionally, previously prepared polypropylene macromonomers have been added to the polymerization of propylene with a metallocene catalyst.[12−14] These methods require careful selection of an isospecific catalyst which can successfully incorporate the polypropylene macromonomers while producing high molecular weight isotactic polypropylene. In several cases, the incorporation of isotactic polypropylene macromonomers was difficult. Branch structure has been identified by the use of SEC with triple detection techniques and ^{13}C NMR. SEC suggested high molecular weight branches, and ^{13}C NMR suggested levels of branching comparable to that of LDPE.

Methods have been developed to produce long chain branches via nonconjugated diene comonomers.[15−18] Incorporated diene monomer provides a reactive functional group along the backbone of polypropylene. Incorporation of this functional group creates a branch point with tetrafunctional structure. Polymers created by this process exhibited broadened molecular weight distributions to values of M_w/M_n greater than 5. Increased zero-shear viscosities were observed through rheological measurements. It has also been shown these branched polymers display strain hardening behavior under elongational flows.[19] At higher concentrations of diene, the storage and loss modulus indicated the formation of a lightly cross-linked network.

* To whom all correspondence should be addressed: e-mail chung@ems.psu.edu.

† Japan Polychem Corporation.

10.1021/ma062111+ CCC: $37.00
Published on Web 03/15/2007

Previously, we prepared branched polypropylenes with relatively well-defined structure by a coupling reaction between chain-end-functionalized polypropylene and polypropylene with graft functionality.[20] The method involves a multiple step postpolymerization process utilizing amine terminated polypropylenes and maleic anhydride graft copolymers of polypropylene. The molecular weight of branches and density of branches were varied. The grafted branch polymers showed a decrease in solution viscosity as compared to their linear counterparts at the same molecular weight. The ratio between branched and linear intrinsic viscosities at the same molecular weight systematically decreased with the increase of both branch density and branch length.

A new, "one-pot" method to synthesize LCBPP via the metallocene-mediated polymerization of propylene with T-reagent was recently reported by our group.[21] This unique procedure allowed for the formation of trifunctional branch points. SEC results suggested the presence of high molecular weight branches. In this paper, we will systematically examine LCBPP polymers with high molecular weight ($M_w \approx 250\,000$ g/mol) produced via this method and provide further evidence of LCB structure. Special attention will be focused on the effects of LCB structure on melt rheology (oscillatory shear and extensional flow) of the resulting LCBPP polymers.

Of significant interest is to study the flow of the LCBPP melts so possible processing benefits can be identified. The melt flow of linear and branched polymers is qualitatively and quantitatively different; therefore, rheology measurements are extremely helpful in determining the presence and nature of branches contained within a material. Rheological studies of monodisperse, branched polyethylene have shown branched polymers of varying architecture displayed relaxation times, zero-shear viscosities, and activation energies which were sensitive to the density of branching, the length of the branches, and molecular weight of the polymer backbone.[22−24] It was found that branched polyethylene had a stronger molecular weight dependence of the zero-shear viscosity, longer relaxation times, and higher activation energies of flow than linear polyethylenes. Additionally, polyethylene showed thermorheological complexity when attempting time−temperature superposition. Similar results have been obtained for long chain branched polypropylenes.[3,6−9,17,18]

Also of rheological importance is the effect of long chain branches on the extensional flow of polymers. It is known that under elongational melt flows LDPE strain-hardens while HDPE with similar zero-shear viscosity does not.[25,26] Linear and branched polypropylenes have been examined in a similar manner.[5,9,27] Polypropylene containing long chain branches strain-hardened while a linear polypropylene did not. These differences in rheology make branched polymers beneficial for some polymer processing operations, such as blow molding and film blowing.

Experimental Section

Instrumentation and Materials. All ^{1}H NMR spectra were recorded on a Bruker AM 300 instrument in 1,1,2,2-tetrachloroethane-d_2 at 110 °C. The melting temperatures of the polymers were measured by differential scanning calorimetry (DSC) using a TA Q100. The melting transitions were recorded during the second heating cycle from 40 to 200 °C with a heating rate of 20 °C/min.

All oxygen- and moisture-sensitive manipulations were carried out inside an argon-filled Vacuum Atmosphere drybox. Toluene (AR grade, from Mallinckrodt) was refluxed over metallic sodium with benzophenone and distilled under nitrogen atmosphere prior to use. *p*-Toluenesulfohydrazide (97%, from Aldrich) was recrystallized from methanol. Vinylbenzyl chloride was vacuum-distilled over calcium hydride. Polymerization-grade propylene (from Matheson Gas) was purified by passage through a column of 4A molecular sieves and calcium carbonate. Allyl magnesium bromide (1.0 M solution in diethyl ether from Aldrich), diethyl ether (anhydrous, from EMD), methylaluminoxane (MAO) (10 wt % solution in toluene from Aldrich), 1,1,2,2-tetrachloroethane-d_2 (99.6% D, from Cambridge Isotope), and 1,3,5-trimethyl-2,4,6-tris-(3,5-di-*tert*-butyl-4-hydroxybenzyl)benzene (99%, from Aldrich) were used as received. *rac*-Dimethylsilanediylbis(2-methyl-4-phenylindenyl)zirconium dichloride was prepared by previously reported methods.[28]

Synthesis of *p*-(3-Butenyl)styrene (T-Reagent). To a dry 500 mL round-bottom flask equipped with addition funnel, condenser, and magnetic stir bar was transferred 200 mL (0.2 mol) of allylmagnesium bromide solution. 20 mL (0.14 mol) of vinylbenzyl chloride diluted with 50 mL of diethyl ether was added dropwise to allylmagnesium bromide at ice bath temperatures. After complete addition, the mixture was warmed to room temperature and stirred for 12 h. Slowly, 200 mL of distilled water was added to the mixture. The aqueous layer was separated and washed three times with diethyl ether. Organic solvent was removed under vacuum. Obtained crude product was dried with calcium hydride and distilled under vacuum before use. Yield: 20.5 g, 93%. ^{1}H NMR ($CDCl_3$, 300 MHz): δ 7.1−7.5 (m, 4H, aromatic H), δ 6.7 (m, 1H, aromatic-CH═C), δ 5.9 (m, 1H, C−CH═C), δ 5.7 (d, 1H, aromatic-C═CH), δ 5.3 (d, 1H, aromatic-C═CH), δ 5.1 (m, 2H, C−C═CH_2), δ 2.7 (t, 2H, aromatic-CH_2), δ 2.4 (m, 2H, CH_2).

Copolymerization of Propylene and *p*-(3-Butenyl)styrene. 100 mL of toluene and 1 mL of MAO solution were added to a dry 300 mL Parr stainless steal autoclave equipped with a mechanical stirrer. The autoclave was then charged with 40 psi of propylene gas, heated to 45 °C, and charged with 1 psi of hydrogen. Propylene gas was used to charge the reaction vessel to a total pressure of 140 psi. 1.1×10^{-7} mol of *rac*-Me_2Si[2-Me-4-Ph-(Ind)]$_2Zr Cl_2$ diluted in 1 mL of toluene and *p*-(3-butenyl)styrene were then injected under propylene pressure. The reaction vessel was stirred and maintained at 55 °C and 140 psi for 30 min. The reaction was terminated by the addition of methanol and cooled to room temperature. The product was washed with acidic methanol and dried under vacuum at room temperature. ^{1}H NMR (1,1,2,2-tetrachloroethane-d_2, 110 °C, 300 MHz): δ 7.1−7.4 (m, aromatic H), δ 2.7 (m, aromatic-CH_2−) δ 1.7 (m, −CH−), δ 1.3 (m, −CH_2−), δ 0.9 (m, CH_3).

Synthesis of Long Chain Branched Isotactic Polypropylene (LCBPP). 100 mL of toluene and 1 mL of MAO solution were added to a dry 300 mL Parr stainless steal autoclave equipped with a mechanical stirrer. The autoclave was then charged with 40 psi of propylene gas, heated to 45 °C, and charged with 1 psi of hydrogen. Propylene gas was used to charge the reaction vessel to a total pressure of 140 psi. 1.1×10^{-7} mol of *rac*-Me_2Si[2-Me-4-Ph(Ind)]$_2Zr Cl_2$ diluted in 1 mL of toluene and *p*-(3-butenyl)styrene were then injected under propylene pressure. The reaction vessel was stirred and maintained at 55 °C and 140 psi for 30 min. The reaction was terminated by the addition of methanol and cooled. The product was washed with acidic methanol, rinsed with methanol, and dried under vacuum at room temperature. ^{1}H NMR (1,1,2,2-tetrachloroethane-d_2, 110 °C, 300 MHz): δ 7.3−7.4 (d, aromatic H), δ 7.1−7.2 (d, aromatic), δ 7.1 (s, aromatic, symmetric), δ 6.7 (m, aromatic-CH═C), δ 5.7 (d, aromatic-C═CH), δ 5.3 (d, aromatic-C═CH), δ 2.7 (t, 2H, aromatic-CH_2), δ 1.7 (m, −CH−), δ 1.3 (m, −CH_2−), δ 0.9 (m, CH_3).

Hydrogenation of LCBPP.[29] To a 250 mL round-bottom flask equipped with condenser and magnetic stir bar was added 1 g of LCBPP, 0.2 g of *p*-toluenesulfohydrazide, 0.08 g of tripropylamine, and 75 mL of toluene. The mixture was brought to a reflux and stirred for 3 h. The mixture was then cooled and washed with methanol. The precipitated polymer was filtered, extracted with methanol for 12 h, and dried in a vacuum oven at 80 °C. Complete hydrogenation of styrene functionality was observed as the disap-

pearance of the ^{1}H NMR peaks at 6.8, 5.7, and 5.2 ppm and the increased intensity of the singlet peak at 7.1 ppm associated with the para-substituted aromatic ring.

Size Exclusion Chromatography. Absolute molecular weight, molecular weight distribution, and viscosity were obtained by SEC with triple detectors at 160 °C using 1,2,4-trichlorobenzene. The chromatographic system consisted of a Polymer Labs PL 220 high-temperature chromatograph equipped with a Precision Detectors two-angle laser light scattering detector model 2040, a Viscotek model 210R viscometer, and a differential refractive index detector. The 15° angle of the light scattering detector was used for calculation purposes. Data collection was performed using Viscotek TriSEC software version 3 and a four-channel Viscotek Data Manager DM400. The system was equipped with an on-line solvent degassing device from Polymer Laboratories.

The chromatographic columns used were three PLgel 10 μm MIXED-B columns obtained from Polymer Laboratories. The solvent used was stabilized 1,2,4-trichlorobenzene. The samples were prepared at a concentration of 0.1 g of polymer in 50 mL of solvent. Both solvent sources were nitrogen sparged. The samples were stirred gently at 160 °C for 2.5 h. The injection volume used was 100 mL, and the flow rate was 1.00 mL/min. The system was calibrated with a standard material (NBS 1475) with a weight-average molecular weight of 52 000 g/mol and an intrinsic viscosity of 1.01 dL/g. The refractive index increment, d*n*/d*c*, was calculated from the calibrated DRI detector as 0.104 mL/g. Molecular weights for the isotactic polypropylene samples were calculated from the intrinsic viscosity detector using the following Mark−Houwink parameters; $K = 1.90 \times 10^{-4}$ dL/g and $a = 0.725$ established for linear isotactic polypropylene from a polystyrene calibration.[30]

Small-Amplitude Dynamic Oscillatory Shear. Rheological measurements were preformed on a strain-controlled Rheometeric Scientific ARES rheometer using a heated stream of nitrogen gas for temperature control. All measurements were preformed under a nitrogen atmosphere, and sample stability was monitored by replicate measurements. 25 mm parallel plates with gap slightly exceeding 1 mm were used. Samples were formed into 25 mm disks by compression-molding. Strain sweeps at frequencies of 1 and 100 rad/s were preformed to ensure measurements were within the linear response region. Frequency sweeps were preformed at five temperatures between 170 and 190 °C in a frequency range of 0.01−100 rad/s.

Extensional Flow Measurements. Extensional flow measurements were made on a strain-controlled TA Instruments ARES rheometer equipped with the extensional viscosity fixture (EVF). Polymer samples were prepared by first gently pressing the polymer into sheet at 200 °C. This sheet was cut and pressed a second time at 10 kg/cm^2 and 200 °C for 10 min, producing a sheet 0.7 mm thick. Samples were cut to the size of 1.0 cm × 1.8 cm and loaded onto the EVF. Tensile stress growth was measured at strain rates varying from 0.005 to 5 s^{-1} at 180 °C.

Results and Discussion

For studying structure−property relationships, a series of LCBPPs (A) with weight-average molecular weights of about 250 000 g/mol and branch point densities ranging from 1 to 3.3 branch points per 10 000 carbons were prepared and compared to a linear PP homopolymer and a random propylene/4-phenylbut-1-ene copolymer (B) prepared under similar reaction conditions. Polymer structures were characterized by ^{1}H NMR spectra and SEC with triple detection. Melt properties were examined by small-amplitude dynamic oscillatory shear and extensional flow measurements.

Synthesis of LCBPP Polymers. Scheme 1 illustrates the reaction mechanism of forming LCBPP polymers via metallocene-mediated propylene polymerization, using isospecific *rac*-Me_2Si[2-Me-4-Ph(Ind)]$_2$ZrCl$_2$/MAO catalyst, in the presence of T-reagent, *p*-(3-butenyl)styrene (BSt), and a small amount of hydrogen. T-reagent serves as both comonomer and

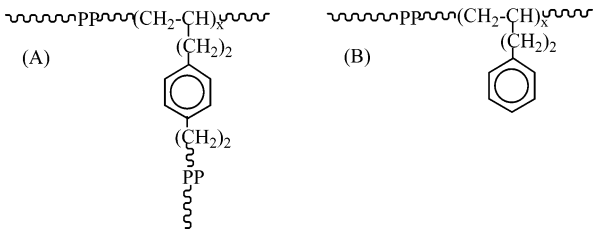

chain transfer agent.[31−34] Copolymerization of the but-3-ene moiety of BSt via 1,2-insertion results in the formation of a copolymer (**III**) with pendant styrene functionality. On the other hand, incorporation of the styrene moiety of BSt via 2,1-insertion results in a dormant catalyst site (**IV**) due to steric hindrance from the bulky aromatic ring and confined catalyst site.[32] Hydrogen can relieve the dormant catalyst site via a subsequent chain-transfer reaction to produce a macromonomer with the α-olefin-like but-3-ene at the chain end. Theoretically, branches in LCBPP (**VI**) can be formed when a growing polymer chain either incorporates the but-3-ene chain end of a macromonomer (**IV**) or chain transfers to the pendant styrene of a copolymer (**III**). As discussed later, the predominate route for the formation of branches involves the pendant styrene of the copolymer (**III**), which serves as the chain transfer agent to form the LCBPP (**VI**) in the presence of hydrogen. The branch point density was proportional to the concentration of T-reagent, and the catalyst maintained high activity due to an effective chain transfer reaction to styrene and then hydrogen. To maintain the high-temperature stability of LCBPP (**VI**), residual pendant styrene units were hydrogenated to form saturated LCBPP (**VII**) for melt rheology study.

One significant concern in this scheme is the direct chain transfer reaction to hydrogen, which will produce linear PP polymer with a reduced molecular weight. It is important to choose a catalyst which is less sensitive to hydrogen and to apply only the required amount of hydrogen to prepare LCBPP. As depicted in Table 1, hydrogen was a necessary component in the process of chain transfer to T-reagent during *rac*-Me_2Si[2-Me-4-Ph(Ind)]Zr_2Cl_2/MAO-mediated propylene polymerization. In PPH1, catalyst activity was almost completely retarded by the addition of a small amount of BSt. 2,1-Insertion of styrene moiety created an inactive site which could no longer incorporate propylene monomer.[30] With the addition of a small amount of hydrogen (1 psi) in PPH2, the catalyst activity returned to expected levels, and the polymer formed was high molecular weight. With an increased amount of hydrogen (PPH3, 10 psi), the molecular weight of the resulting polymer was reduced. At this high hydrogen concentration, direct chain transfer to hydrogen became a significant side reaction. Therefore, for the preparation of LCBPPs it is important to use only minimum amounts of hydrogen, such that chain transfer via hydrogen does not compete with chain transfer to T-reagent.

The chemical structures of the obtained materials were examined by ^{1}H NMR (Figure 1). The structures of copolymer and macromonomer could be identified by their unique chemical shifts. Copolymer containing pendant styrene functionality was observed by three vinyl protons with chemical shifts at 6.8, 5.7, and 5.2 ppm, while macromonomer was observed by three vinyl protons at 5.9 and 5.1 ppm. Branch points created by the combination of copolymerization and chain transfer of/to BSt were identified by comparing the aromatic protons with a chemical shift of 7.1 ppm with the amount of macromonomer observed. Macromonomer only accounted for a minor amount of the aromatic protons at 7.1 ppm, leaving branch points as the major contributor. Low levels or lack of macromonomer

Scheme 1

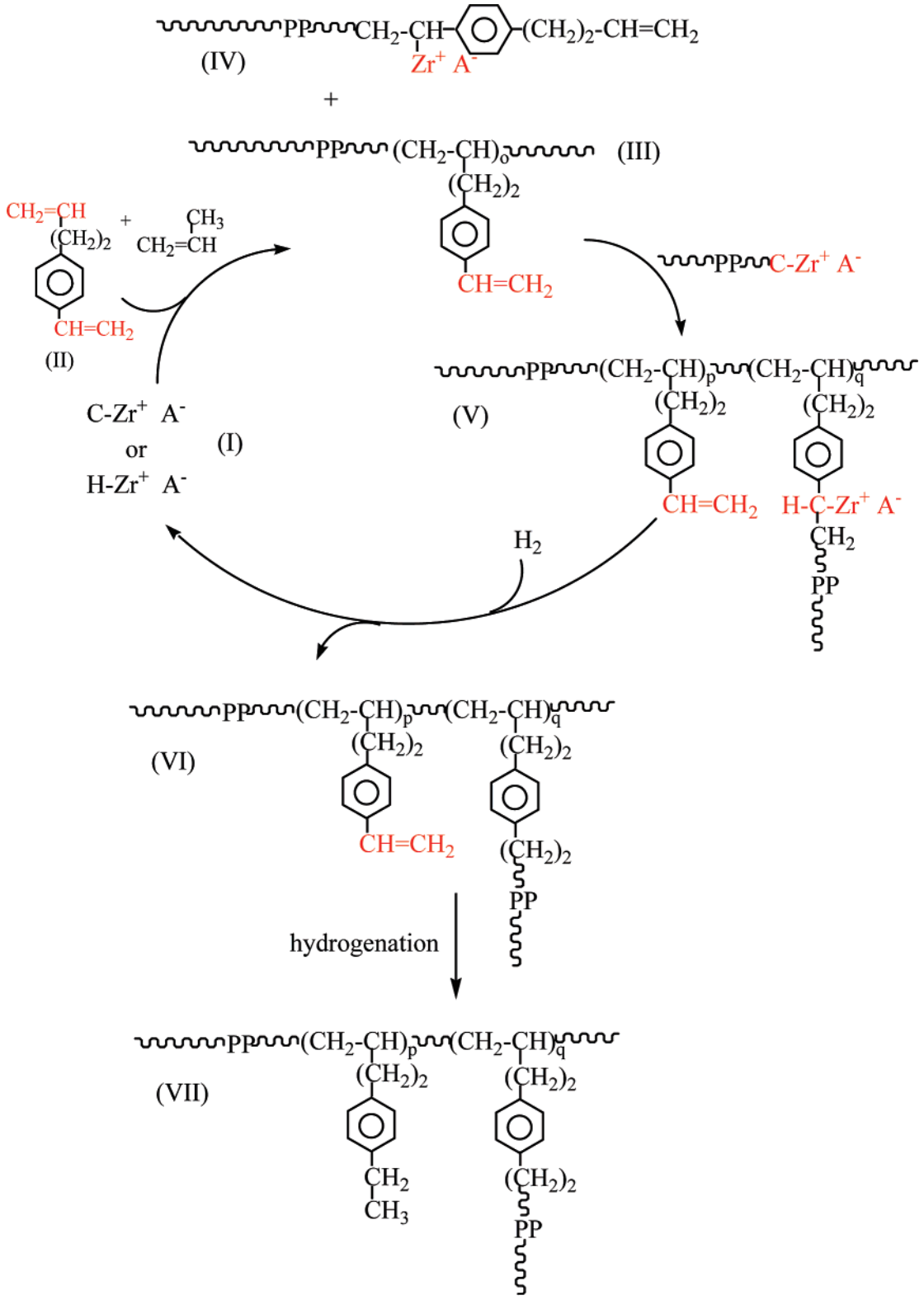

structure suggested either the produced macromonomers with vinyl-terminated chain end were incorporated into LCBPP at high conversions or incorporation of BSt highly preferred insertion of the but-1-ene moiety. The latter should be the preferred explanation because the incorporation of highly crystalline, high molecular weight PP macromonomer should be very difficult under these heterogeneous conditions.

Table 2 summarizes the results of several polymerization reactions using various amounts of T-reagent (BSt). Catalyst activities of LCBPP1 and LCBPP2 were comparable to both the homopolymerization of propylene and the copolymerization of propylene with 4-phenylbut-1-ene. With higher BSt concentrations in LCBPP3 and LCBPP4, the catalyst activity was proportionally reduced, which may be associated with the slow down in chain transfer reaction to T-reagent/H_2. The branch point density was calculated from ^{1}H NMR spectra. The branch point density was proportional to the feed concentration of BSt and increased from LCBPP1 to LCBPP4. It is interesting to

Table 1. Experimental Results of *rac*-Me_2Si[2-Me-4-Ph(Ind)]Zr_2Cl_2/MAO-Mediated Propylene Polymerizations in the Presence of T-Reagent (0.007 mol/L) and Various Hydrogen Pressures

sample	hydrogen [psi]	catalyst activity [kg of PP/(mmol of Zr•h)]	$M_{w,LS}$[a] [g/mol]
PPH1	0	20	n/a[b]
PPH2	1	225	232 500
PPH3	10	330	45 000

[a] Measured by SEC with dynamic light scattering detector. [b] Not measured.

note that on average 43% of the incorporated T-reagent was associated with branch structure, independent of BSt concentration and reaction time. LCBPP4 was run twice as long as LCBPP3 but contained similar ratios between the amounts of pendant styrene and branch points observed. These results may imply that copolymerized T-reagent was immediately involved in a chain transfer reaction to form a branch point before the polymer precipitated from solution and the incorporated BSt units became inaccessible. Melting temperature, T_m, of LCBPP samples, examined by DSC, showed a gradual reduction of T_m with increase of branch density.

Size Exclusion Chromatography with Triple Detection. Figure 2 shows molecular weight distribution curves of linear and LCBPP samples, which were examined by SEC with triple detectors. The weight-average molecular weights determined by light scattering, $M_{w,LS}$, are displayed in Table 2. Compared with iPP homopolymer (PP1), $M_{w,LS}$ decreased with the addition of comonomer (PP2) and initially with the addition of BSt (LCBPP1). Further addition of BSt increased $M_{w,LS}$ only slightly. Hence, all four LCBPPs have a $M_{w,LS}$ of about 250 000 g/mol. The polydispersity index, M_w/M_n, of all the resulting polymers remained below 3.

Size exclusion chromatography with triple detectors (refractive index, intrinsic viscosity, and light scattering) can detect differences between the hydrodynamic volume of linear and branched polymers.[35,36] Simultaneous measurement of intrinsic viscosity, $[\eta]$, and absolute molecular weight, M_{LS}, for each fraction of polymer separated by the chromatography columns can provide interesting information about the structure of branched polymers. Mark−Houwink plots, log−log plots of intrinsic viscosity vs absolute molecular weight for each slice of the SEC elution, can be used to qualitatively observe branching. Figure 3 shows the Mark−Houwink plots of the LCBPPs with respect to a linear standard. The linear standard behaved in a fashion described by the Mark−Houwink relation (eq 1), where K and a can be obtained from the slope and intercept of the Mark−Houwink plot.

$$[\eta] = KM^a \tag{1}$$

The linear isotactic polypropylene had a single slope of $a = 0.725$. Branched polymers began to deviate from linear behavior at high molecular weights. The slopes of the Mark−Houwink plot for the LCBPPs deviated for that of the linear standard. The deviation from linear behavior was subtle at low branch point density but became more apparent as branch point density was increased. The largest change in slope to $a = 0.28$ was observed for LCBPP4 containing the highest content of branch points. The effective molecular weight, M_x, between long branches can be obtained from locating the intersection of linear and branched behavior. For all samples, M_x was ~500 000 g/mol, which is several times larger than M_w. These values of M_x suggested most of the branches existed in the high molecular weight fraction of the polymer.

Additional support for long chain branching was observed through the branching parameter, g' (eq 2), where $[\eta]_B$ was obtained as a weight-average from the SEC experiments and $[\eta]_L$ was calculated using Mark−Houwink parameters of $K = 1.901 \times 10^{-4}$ dL/mol and $a = 0.725$. For the linear samples PP1 and PP2, g' was unity. For the LCBPPs, g' was less than one and decreased with increased branch density.

$$g' = \frac{[\eta]_B}{[\eta]_L} \tag{2}$$

Figure 4 depicts the Mark−Houwink plots for two LCBPPs and a linear iPP. The two LCBPPs were prepared with 2 and 10 psi of hydrogen. The deviation of the slope from unity in both LCBPP plots starts at low molecular weight and gradually increases with the increase of polymer molecular weight, which implies a uniform branch distribution along the LCBPP chain, and only a small portion of low molecular weight polymers are linear, without branching. The M_x and a of the two LCBPPs remained similar despite a reduction of M_w by 42% for the sample prepared with 10 psi of hydrogen. These results suggested that the structure of the branched material was unaffected by the increased concentration of hydrogen; namely, M_x remained essentially unchanged. Although the structure of the branched material was unaffected, the higher concentration of hydrogen decreased the concentration of branched material. ^{1}H NMR further clarified the effect of hydrogen on the samples, 56% of the incorporated BSt produced a branch point for the 2 psi LCBPP, while only 49% produced branch points in the 10 psi LCBPP. Direct transfer to hydrogen competed with chain transfer to pendant styrene groups.

Small-Amplitude Dynamic Oscillatory Shear. Oscillatory shear measurements were obtained at five temperatures between 170 and 190 °C. Figure 5a shows the master curves of storage and loss modulus obtained by time−temperature superposition for PP1. The linear sample showed characteristic behavior of a viscoelastic material in the Newtonian (terminal) region. At higher frequencies a crossover of G' and G'' was observed. At lower frequencies G' and G'' became proportional to ω^2 and ω, respectively. Branched polymers (represented by LCBPP4 in Figure 5b) had longer relaxation times, and the proportionality of G' and G'' to ω^2 and ω was not observed at the lowest frequencies measured. These results were consistent with the SEC results, which suggested significant branching in the high molecular weight region of the distribution.

Figure 6 shows the storage moduli for LCBPPs and PP2. Linear PP2 with similar molecular weight to that of the LCBPPs behaved as expected with the slope of G' approaching 2 at low frequency. However, the LCBPPs were observed to have broadened storage moduli with slopes only approaching values of 1.5 at the lowest frequencies measured, indicating the relaxation times increased as the branch density of the polymers increased.

Additional evidence of branched structure was observed by the failure of time−temperature superposition for long chain branched samples. Time−temperature superposition worked well for LCBPP1 and LCBPP2 with low branch point densities, but sample LCBPP3 and specifically sample LCBPP4 showed poor time−temperature superposition. Figure 7 shows an attempted time−temperature superposition of LCBPP4. The loss tangent, $\tan(\delta)$, demonstrates unambiguously the poor superposition, as no vertical scale shifting is allowed for $\tan(\delta) \equiv G''/G'$, as it is a ratio of moduli.

Failure of time−temperature superposition is characteristic of a thermorheologically complex material. Most commonly,

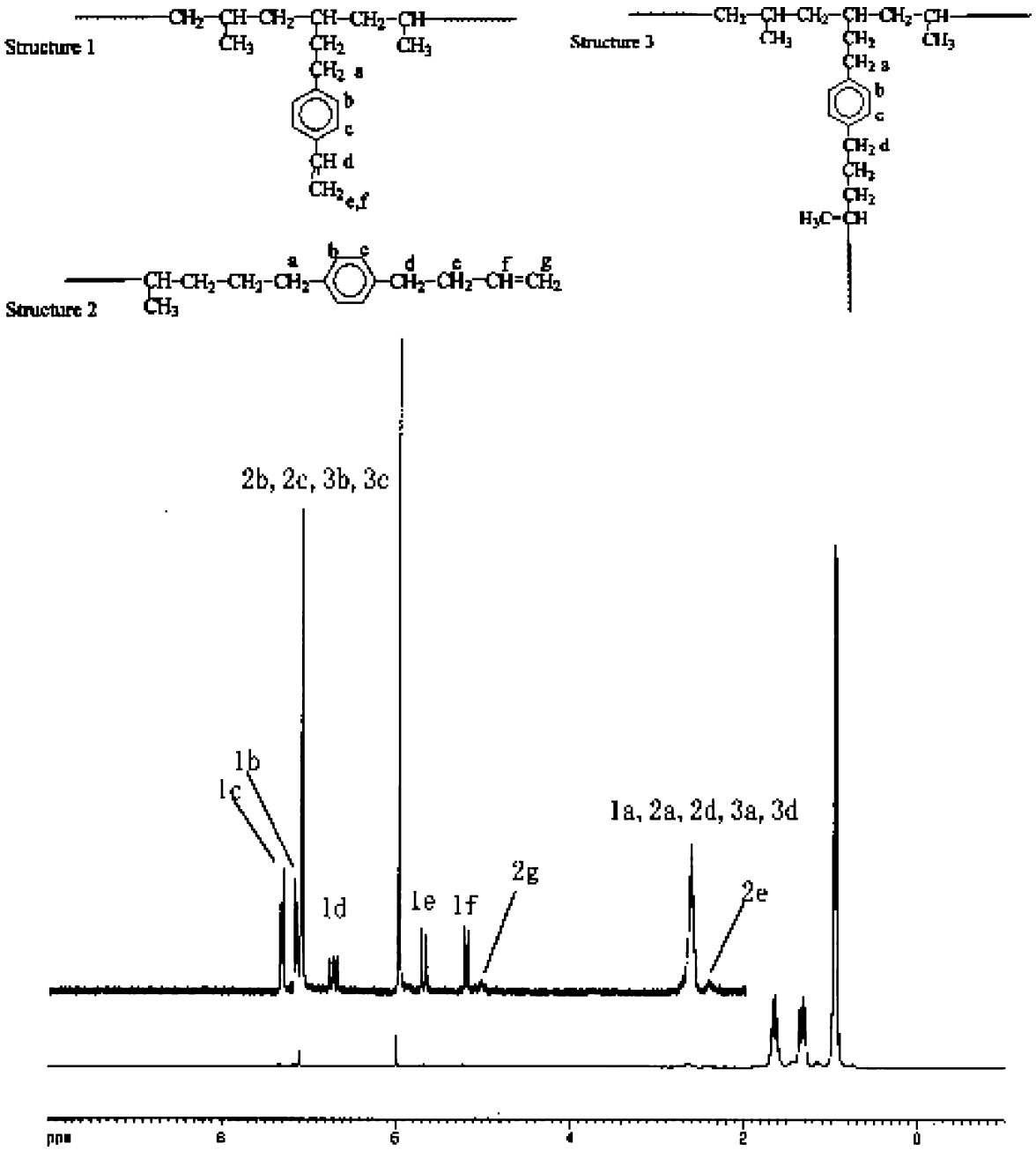

Figure 1. Representative ^{1}H NMR spectrum of a LCBPP polymer in tetrachloroethane-d_2 at 110 °C with assignments.

Table 2. Comparison of Linear and LCBPP Polymers Prepared by *rac*-Me$_2$Si[2-Me-4-Ph(Ind)]Zr$_2$Cl$_2$/MAO-Mediated Propylene Polymerizations

sample	[BSt] (mol/L)	cat. act.[a]	$M_n/M_{w,VIS}$[b] ($\times 10^3$ g/mol)	$M_n/M_{w,LS}$[c] ($\times 10^3$ g/mol)	F_{BSt}[d] (mol %)	$[\eta]$[e] (dL/g)	g'[f]	branch den[g]	$\eta_{0,190°C}$ (Pa·s)	E_a (kJ/mol)	M_b[h] (g/mol)	T_m (°C)
PP1	0.000	210	167/443	160/430	0.00	2.283	0.99	0.0	17250	39	linear	158
PP2[i]	0.013[j]	190	104/255	95/248	0.15[k]	1.542	1.00	0.0	1030	40	linear	155
LCBPP1	0.007	225	91/238	94/249	0.07	1.485	0.96	1.0	3200	48	246 000	157
LCBPP2	0.013	190	91/240	91/240	0.13	1.412	0.91	1.8	3890	49	232 000	155
LCBPP3	0.020	100	96/238	94/247	0.15	1.385	0.92	2.2	5700	50	235 000	153
LCBPP4	0.030	64	87/238	87/256	0.21	1.370	0.87	3.3	9030	61	238 200	153

[a] Catalyst activity: [kg of PP/(mmol of Zr·h)]. [b] Measured by SEC with universal calibration of the viscosity detector. [c] Measured by SEC with light scattering detector. [d] Mol % of incorporated BSt. [e] Weight-average intrinsic viscosity obtained from SEC with viscosity detector. [f] Ratio of branched intrinsic viscosity to linear intrinsic viscosity at the same average molecular weight, $g' = [\eta]_B/[\eta]_L$, where $[\eta]_B$ is the weight-average intrinsic viscosity and $[\eta]_L$ is calculated from the Mark−Houwink parameters $K = 1.901 \times 10^{-4}$ dL/g and $a = 0.725$ using $M_{w,LS}$. [g] ^{1}H NMR branch density: [branch points/10 000 carbon]. [h] Calculated from melt viscosity using the Janzen−Colby model. [i] Linear copolymer of propylene and 4-phenylbut-1-ene. [j] Concentration of 4-phenylbut-1-ene. [k] Mol % of incorporated 4-phenylbut-1-ene.

this behavior has been attributed to branched polyethylenes and has been suggested to depend strongly on the temperature coefficient of chain dimensions.[37] Polymers with sufficient branch density and large negative temperature coefficients of chain dimensions are anticipated to be thermorheologically complex. Atactic polypropylene has a temperature coefficient of chain dimensions of -0.1×10^{-3} K^{-1},[38] while polyethylene has a temperature coefficient of chain dimensions of $-1.05 \times$

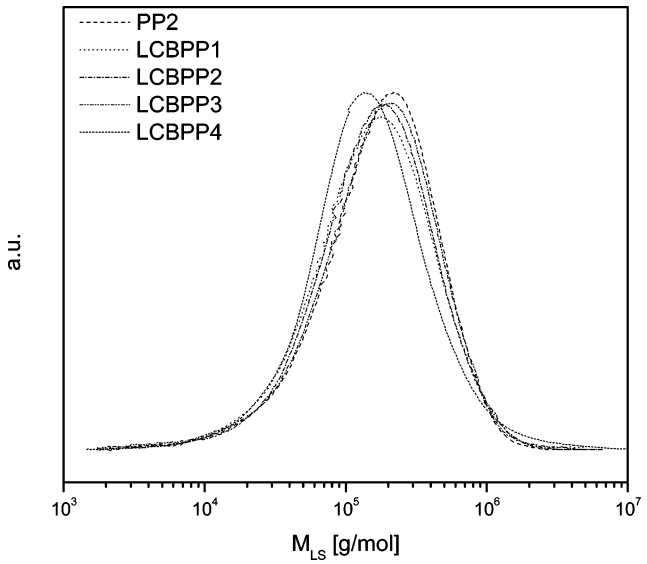

Figure 2. Absolute molecular weight distributions of linear and LCBPPs determine by light scattering detector.

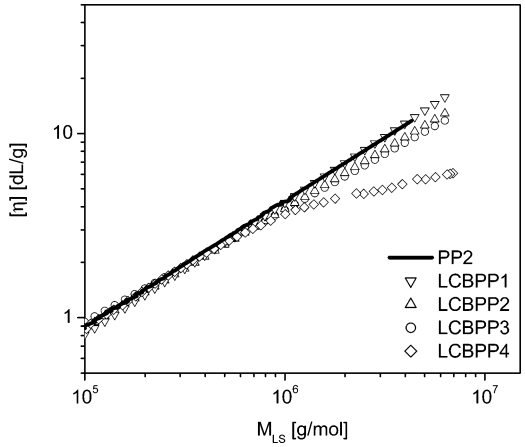

Figure 3. Mark−Houwink plot of linear PP (solid line) and LCBPPs.

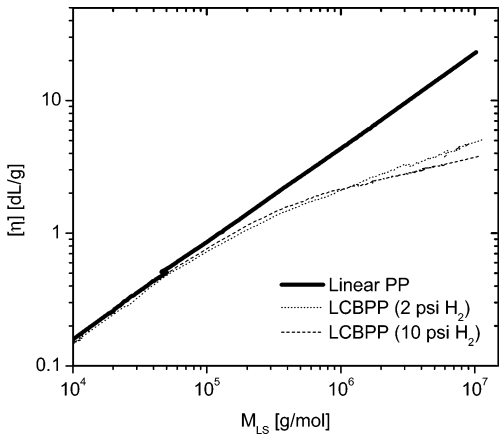

Figure 4. Mark−Houwink plot of linear PP (solid line) and LCBPPs prepared with 2 and 10 psi of hydrogen.

10^{-3} K^{-1}.[39] The temperature coefficient of chain dimensions for polypropylene is negative, but small in comparison to the coefficient for polyethylene. Failure of time−temperature superposition in branched polypropylenes was less dramatic as what has been reported for branched polyethylene, which could possibly be due to the difference in magnitude of the temperature dependence of chain dimensions. Therefore, the observed thermorheological behavior for the branched polypropylenes is

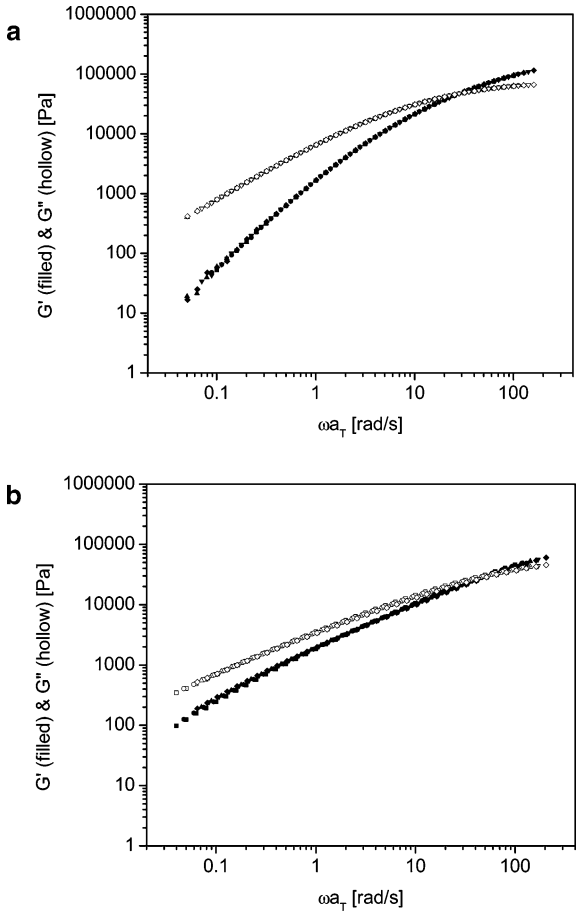

Figure 5. Master curves of storage and loss moduli at 190 °C: (a) linear PP1, (b) LCBPP4.

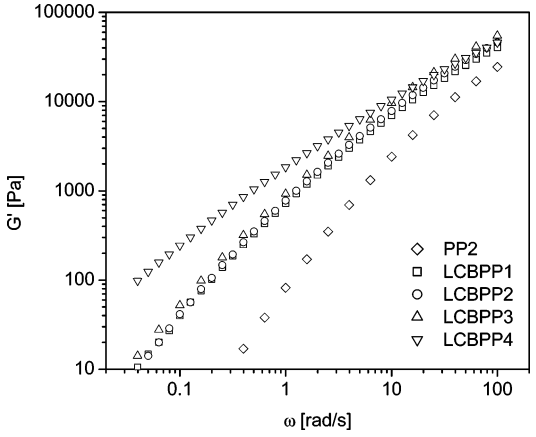

Figure 6. Storage moduli for linear PP2 and LCBPPs at 190 °C.

in agreement with the hypothesis of Graessley.[37] Additionally, the results suggest LCBPP4 contained high molecular weight branches of significant branch density.

The complex viscosities of the LCBPPs and PP2 are presented in Figure 8. The complex viscosity, η^*, and particularly zero-shear viscosity, η_0, are extremely sensitive to branching. The molecular weight of PP2 was similar to those of the LCBPPs, but the zero-shear viscosities of the LCBPPs were considerably higher than that of linear PP2. Additionally, LCBPPs had broader transitions from shear-thinning behavior at higher frequencies to Newtonian behavior at low frequencies, consistent with broader distributions and branching. Newtonian behavior was harder to obtain in LCBPPs as is clearly illustrated by sample LCBPP4's lack of a frequency-independent viscosity

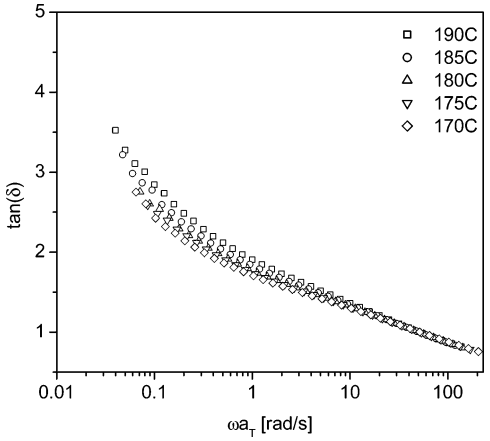

Figure 7. Attempted time−temperature superposition of LCBPP4. Data were superimposed at high frequency. Reference temperature is 190 °C.

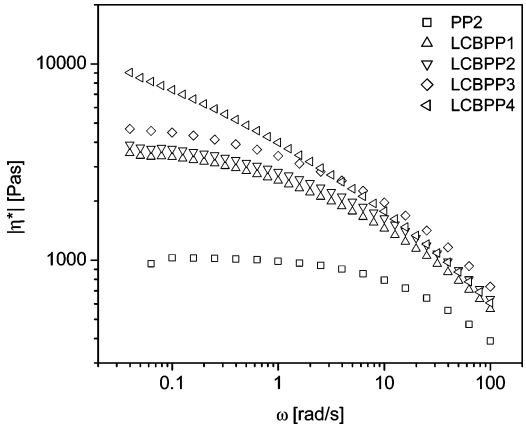

Figure 8. Magnitude of complex viscosities for various isotactic polypropylenes at 190 °C.

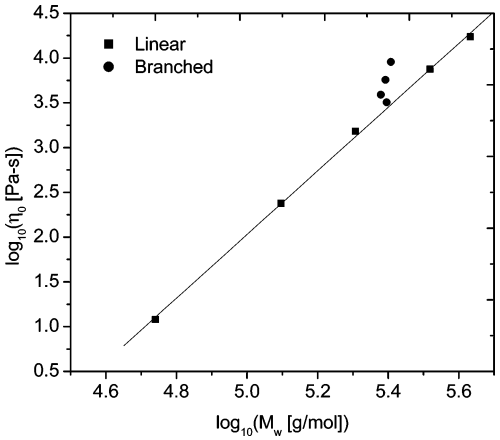

Figure 9. Relationship of zero-shear viscosity at 190 °C and weight-average molecular weight for linear and branched isotactic polypropylenes. Line is eq 5.

in the frequency range measured. This behavior can be attributed to the long relaxation times of branched polymers.

$$\eta_0 \propto M_w^{1} \qquad \text{for } (M_w < M_c) \tag{3}$$

$$\eta_0 \propto M_w^{3.4} \qquad \text{for } (M_w > M_c) \tag{4}$$

$$\eta_0 = 1.77 \times 10^{-16} M_w^{3.56} \quad \text{(Pa·s, 190 °C)} \tag{5}$$

Figure 10 shows the log−log plot of zero-shear viscosity and

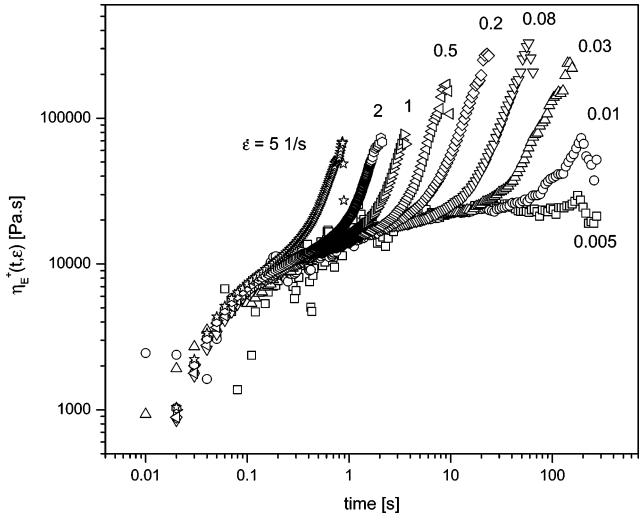

Figure 10. Extensional stress growth function at various strain rates for LCBPP4 at 180 °C.

weight-average molecular weight. The zero-shear viscosity of a linear polymer is expected to follow eqs 3 and 4, where M_c is the critical molecular weight for entanglements or approximately twice the molecular weight between entanglements, M_e. The five linear isotactic polypropylenes followed the expected behavior for entangled melts[40] and could be described by eq 5, but the branched polymers deviated from this behavior. For branched samples the zero-shear viscosity was more sensitive to molecular weight. The zero-shear viscosity of LCBPP4 was nearly 3 times the zero-shear viscosity of the linear polymer of the same M_w.

$$\eta_0 = AM_b\left[1 + \left(\frac{M_b}{M_c}\right)^{2.4}\right]\left(\frac{M_w}{M_c}\right)^{s/\gamma} \tag{6}$$

$$s/\gamma = \max\left[1, \frac{3}{2} + \frac{9}{8}B\ln\left(\frac{M_b}{90M_{Kuhn}}\right)\right] \tag{7}$$

$$\eta_0 = AM_w\left[1 + \left(\frac{M_w}{M_c}\right)^{2.4}\right] \tag{8}$$

Utilizing the measured zero-shear viscosities and absolute weight-averaged molecular weights of the LCBPPs, the average molecular weight between branches, M_b, was calculated using a model proposed by Janzen and Colby.[41] M_b was obtained from eqs 6 and 7, with $M_c = 2M_e = 13\,640$ g/mol, $M_{Kuhn} = 187.8$ g/mol, $B = 6$, and $A = 1.02 \times 10^{-5}$ calculated from fitting several linear polymers to eq 8. Table 2 contains the results for M_b of the LCBPPs. The calculated M_b slightly decreased with increasing branch density. An M_b of slightly less than M_w suggested sparse branching with high molecular weight branches, which agreed with SEC results.

$$a_T = \exp\left[\frac{E_a}{R}\left(\frac{1}{T} - \frac{1}{T_0}\right)\right] \tag{9}$$

The Arrhenius activation energy for flow, E_a, can be determined using the frequency scale shift factors obtained from the time−temperature superposition of the oscillatory shear data at several temperatures from eq 8. Arrhenius activation energies for flow are listed in Table 2. Even LCBPP1 with the lowest levels of branching showed a significant increase in flow activation energy. The systematic increase in Arrhenius activation energy for flow with branch density can be attributed to

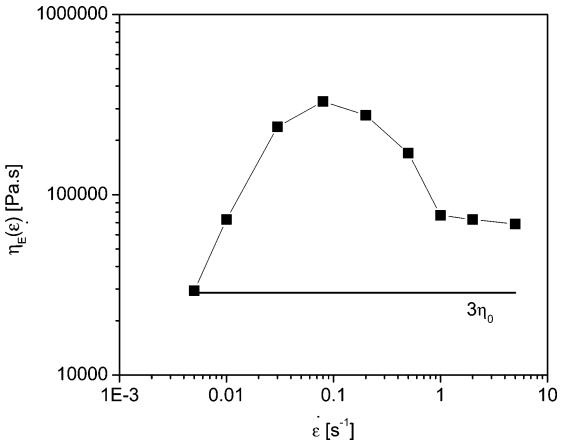

Figure 11. Extensional viscosity vs strain rate for LCBPP4 at 180 °C. Solid line corresponds to 3 times the zero-shear viscosity obtained from small-amplitude oscillatory shear.

the long chain branched structure.[42] LCBPP4 with the highest branch density had a flow activation energy higher than the linear standards and branched polypropylenes prepared by electron beam irradiation (48 kJ/mol) or diene comonomer (42 kJ/mol) methods.[19]

Extensional Flow. An examination of the extensional flow characteristics of LCBPP4 was performed using an ARES rheometer equipped with the extensional viscosity fixture. The extensional stress growth function, $\eta_E^+(t,\dot{\epsilon})$, is shown in Figure 10 at various Hencky extension rates, $\dot{\epsilon}$, for LCBPP4. At each extension rate there existed a range of deformation which perfectly tracked linear viscoelastic response. Additionally, at all extension rates studied, with perhaps the exception of $\dot{\epsilon} = 0.005$ s^{-1}, strain hardening was observed. Strain hardening was observed as a sharp increase of $\eta_E^+(t,\dot{\epsilon})$ above the values at $\dot{\epsilon} = 0.005$ s^{-1}. Such strain hardening is believe to be important for polymer processing operations requiring high melt strength, such as fiber spinning and film blowing.[1]

Extensional viscosities, $\eta_E(\dot{\epsilon})$, were obtained from the maximum values of the stress growth functions at each $\dot{\epsilon}$ and are plotted against $\dot{\epsilon}$ in Figure 11. Trouton's rule predicts $\eta_E(\dot{\epsilon}) = 3\eta(\dot{\gamma})$.[43] At the lowest strain rate the melt behaved as a linear viscoelastic liquid and the extensional viscosity was 3 times the zero-shear viscosity within experimental uncertainties. At higher strain rates the extensional viscosity increased with increasing strain rate and reached a maximum value of $\eta_E(\dot{\epsilon}) = 11.5(3\eta_0)$ at a Hencky rate of 0.08 s^{-1}. At Hencky rates above 0.08 s^{-1} the extensional viscosity decreased with increasing strain rate. The extensional flow properties of polymer melts were extremely sensitive to the presence of branches, with results similar to those obtained for LCBPP4 having been reported.[44]

Conclusion

LCBPP was produced by the metallocene-mediated polymerization of propylene and T-reagent. T-reagent effectively acts as both a comonomer and a chain transfer agent and required hydrogen to complete chain transfer. Branch point densities of the resulting materials were controlled by the concentration of BSt and were verified by ^{1}H NMR. SEC with triple detection depicted branched structures with high molecular weight branches in the high molecular weight tail of the distribution. Branch densities affected the slope of the Mark−Houwink plot in the high molecular weight range. Small-amplitude oscillatory shear showed control of branch point density allowed for the synthesis of LCBPPs with varying zero-shear viscosities, relaxation times, and Arrhenius activation energies for flow. LCBPP was observed to behave as a strain hardening material under extensional flow, useful for polymer processing operations requiring stability in extension.

Acknowledgment. The authors thank Mitsubishi Chemical Co. and the Office of Naval Research for financial support. Authors also thank Mr. Drew Poche for performing SEC.

References and Notes

(1) Dealy, J. M.; Wissbrun, K. F. *Melt Rheology and its Role in Pastics Processing: Theory and Applications;* Kluwer Academic: Dordrecht, The Netherlands, 1999.
(2) Xiaochun, W.; Tzoganakis, C.; Rempel, G. L. *J. Appl. Polym. Sci.* **1996**, *61*, 1395.
(3) Graebling, D. *Macromolecules* **2002**, *35*, 4602.
(4) Sheve, B. J.; Mayfield, J. W.; Denicola, A. J. US Patent 4,916,198, 1990.
(5) Yoshii, F.; Makuuchi, K.; Kikukawa, S.; Tanaka, T.; Saitoh, J.; Koyama, K. *J. Appl. Polym. Sci.* **1996**, *60*, 617.
(6) Auhl, D.; Stange, J.; Munstedt, H.; Krause, B.; Voigt, D.; Lederer, A.; Lappan, U.; Lunkwitz, K. *Macromolecules* **2004**, *37*, 9465.
(7) Hingmann, R.; Marczinke, B. *J. Rheol.* **1994**, *38*, 573.
(8) Sugimoto, M.; Masubuchi, Y.; Takimoto, J.; Koyama, K. *J. Appl. Polym. Sci.* **1999**, *73*, 1493.
(9) Kurzbeck, S.; Oster, F.; Münstedt, H.; Nguyen, T. Q.; Gensler, R. *J. Rheol.* **1999**, *43*, 359.
(10) Weng, W.; Hu, W.; Dekmerzian, A. H.; Ruff, C. J. *Macromolecules* **2002**, *35*, 3838.
(11) Ye, Z.; Zhu, S. *J. Polym. Sci., Part A: Polym. Chem.* **2003**, *41*, 1152.
(12) Shiono, T.; Azad, S. M.; Ikeda, T. *Macromolecules* **1999**, *32*, 5723.
(13) Weng, W.; Markel, E. J.; Dekmerzian, A. H. *Macromol. Rapid Commun.* **2000**, *21*, 103.
(14) Cherian, A. E.; Lobkovsky, E. B.; Coates, G. W. *Macromolecules* **2005**, *38*, 6259.
(15) Meka, P.; Kunihiko, I.; Licciardi, G. F.; Gadkari, A. C. U.S. Patent 5,670,595, 1997.
(16) Rosch, J.; Mach, H.; Gruber, F. U.S. Patent 5,929,185, 1999.
(17) Paavola, S.; Saarinena, T.; Löfgren, B.; Pitkänen, P. *Polymer* **2004**, *45*, 2099.
(18) Ye, Z.; Alobaidi, F.; Zhu, S. *Ind. Eng. Chem. Res.* **2004**, *43*, 2860.
(19) Sugimoto, M.; Suzuki, Y.; Hyun, K.; Ahn, K. H.; Ushioda, T.; Nishioka, A.; Taniguchi, T.; Koyama, K. *Rheol. Acta*, in press.
(20) Lu, B.; Chung, T. C. *Macromolecules* **1999**, *32*, 8678.
(21) Langston, J.; Dong, J. Y.; Chung, T. C. *Macromolecules* **2005**, *38*, 5849−5853.
(22) Rachapudy, H.; Smith, G. G.; Raju, V. R.; Graessley, W. W. *J. Polym. Sci. Phys.* **1979**, *17*, 1211.
(23) Carella, J. M.; Gotro, J. T.; Graessley, W. W. *Macromolecules* **1986**, *19*, 659.
(24) Lohse, D. J.; Milner, S. T.; Fetters, L. J.; Xenidou, M.; Hadjichristidis, N.; Mendelson, R. A.; Garcia-Franco, C. A.; Lyon, M. K. *Macromolecules* **2002**, *35*, 3066.
(25) Münstedt, H.; Laun, H. M. *Rheol. Acta* **1981**, *20*, 211.
(26) Meissner, J. *Chimia* **1984**, *38*, 65.
(27) Gabriel, C.; Münstedt, H. *J. Rheol.* **2003**, *47*, 619.
(28) Spalek, W.; Küber, F.; Winter, A.; Rohrmann, J.; Bachmann, B.; Antberg, M.; Dolle, V.; Paulus, E. F. *Organometallics* **1994**, *13*, 954.
(29) Hahn, S. F. *J. Appl. Polym. Sci., Part A: Polym. Chem.* **1992**, *30*, 397.
(30) Williams, T.; Ward, I. M. *J. Polym. Sci., Polym. Lett.* **1968**, *6*, 621.
(31) Chung, T. C.; Dong, J. Y. U.S. Patent 6,479,600, 2002.
(32) Chung, T. C.; Dong, J. Y. *J. Am. Chem. Soc.* **2001**, *123*, 4871.
(33) Dong, J. Y.; Chung, T. C. *Macromolecules* **2002**, *35*, 1622.
(34) Dong, J. Y.; Wang, Z. M.; Han, H.; Chung, T. C. *Macromolecules* **2002**, *35*, 9352.
(35) Zimm, B. H.; Stockmayer, W. H. *J. Chem. Phys.* **1949**, *17*, 1301.
(36) Billmeyer, Jr., F. W. *J. Am. Chem. Soc.* **1953**, *75*, 6118.
(37) Graessley, W. W. *Marcomolecules* **1982**, *15*, 1164.
(38) Zirkel, A.; Urban, V.; Richter, D.; Fetters, L. J.; Huang, J. S.; Kampmann, R.; Hadjichristidis, N. *Macromolecules* **1992**, *25*, 6148.
(39) Mark, J. E. *J. Polym. Sci., Macromol. Rev.* **1976**, *11*, 135.
(40) Wasserman, S. H.; Graessley, W. W. *Polym. Eng. Sci.* **1996**, *36*, 852.
(41) Janzen, J.; Colby, R. H. *J. Mol. Struct.* **1999**, *485−486*, 569.
(42) Graessley, W. W. *Acc. Chem. Res.* **1977**, *10*, 332.
(43) Trouton, F. T. *Proc. R. Soc. London A* **1906**, *77*, 426.
(44) Laun, H. M.; Münstedt, H. *Rheol. Acta* **1978**, *17*, 415.

MA062111+